Morphogenesis of Maize Embryos Requires *ZmPRPL35-1* Encoding a Plastid Ribosomal Protein[1]

Jean-Louis Magnard[2], Thierry Heckel[3], Agnès Massonneau, Jean-Pierre Wisniewski, Sylvain Cordelier, Hervé Lassagne, Pascual Perez, Christian Dumas, and Peter M. Rogowsky*

Reproduction et Développement des Plantes, Unité Mixte de Recherche 5667, Institut National de la Recherche Agronomique-Centre National de la Recherche Scientifique-Ecole Normal Supérieure de Lyon-Université Claude Bernard Lyon I, Institut Fédératif de Recherche 128 BioSciences Lyon-Gerland, Ecole Normale Supérieure-Lyon, 46 Allée d'Italie, F–69364 Lyon cedex 07, France (J.-L.M., T.H., A.M., J.-P.W., C.D., P.M.R.); and Biogemma, Laboratoire de Biologie Cellulaire et Moléculaire, Campus Universitaire des Cézeaux, 24 Avenue des Landais, F–63177 Aubière, France (S.C., H.L., P.P.)

In *emb* (*embryo specific*) mutants of maize (*Zea mays*), the two fertilization products have opposite fates: Although the endosperm develops normally, the embryo shows more or less severe aberrations in its development, resulting in nonviable seed. We show here that in mutant *emb8516*, the development of mutant embryos deviates as soon as the transition stage from that of wild-type siblings. The basic events of pattern formation take place because mutant embryos display an apical-basal polarity and differentiate a protoderm. However, morphogenesis is strongly aberrant. Young mutant embryos are characterized by protuberances at their suspensor-like extremity, leading eventually to structures of irregular shape and variable size. The lack of a scutellum or coleoptile attest to the virtual absence of morphogenesis at the embryo proper-like extremity. Molecular cloning of the mutation was achieved based on cosegregation between the mutant phenotype and the insertion of a *MuDR* element. The *Mu* insertion is located in gene *ZmPRPL35-1*, likely coding for protein L35 of the large subunit of plastid ribosomes. The isolation of a second allele *g2422* and the complementation of mutant *emb8516* with a genomic clone of *ZmPRPL35-1* confirm that a lesion in *ZmPRPL35-1* causes the *emb* phenotype. *ZmPRPL35-1* is a low-copy gene present at two loci on chromosome arms 6L and 9L. The gene is constitutively expressed in all major tissues of wild-type maize plants. Lack of expression in *emb/emb* endosperm shows that endosperm development does not require a functional copy of *ZmPRPL35-1* and suggests a link between plastids and embryo-specific signaling events.

Plant embryogenesis is a complex developmental process characterized by three major events: (a) establishment of an apical/basal pattern; (b) radial differentiation in epidermis, ground tissue, and vascular tissue; and (c) the formation of shoot and root meristems (Kaplan and Cooke, 1997). Numerous mutants with defects in various aspects of embryo development have been characterized, and several of the underlying genes have been cloned in the model species Arabidopsis (Jürgens, 2001). In maize (*Zea mays*), efforts have focused mainly on two type of mutants: *dek* (*defective kernel*) mutants are affected both in embryo and endosperm development (Neuffer and Sheridan, 1980; Sheridan and Neuffer, 1980), whereas *emb* (*embryo specific*) mutants exhibit aberrant embryo but normal endosperm development (Clark and Sheridan, 1991; Sheridan and Clark, 1993). Two *Dek* genes have been cloned. *Lachrima* (*DekB*) encodes a novel transmembrane protein possibly involved in auxin transport (Stiefel et al., 1999), and *Dek1*, a member of the calpain family, is involved in signal transduction (Lid et al., 2002). So far, no cloning of an *Emb* gene has been reported, and the reasons for their specific action on embryo development remain to be elucidated.

Embryo and endosperm are the two products of the double fertilization event typical of higher plants. The embryo results from the fusion of the egg cell with a first sperm cell, and the endosperm is the fusion product of the central cell with a second sperm cell. In terms of evolution, the embryo and the endosperm have very similar origins because the endosperm is thought to have evolved from a supernumerary embryo (Friedman, 1994). In the plants of today, they have rather different structure and function. The embryo is a highly differentiated structure that never looses its totipotency and continues its development after germination to form the vegetative apparatus and eventually a mature plant. The endosperm is essentially a storage tissue that stops its growth sooner or later to undergo programmed cell death and to provide nutrients to the embryo (Young

[1] This work was supported in part by the European Commission (contract no. BIO4–CT96–0210) and by Biogemma SA (to T.H. and J.L.M.).

[2] Present address: Biotechnologies Végétales, Université Jean Monnet, 23 Rue du Docteur Paul Michelon, F-42023 Saint-Etienne cedex 02, France.

[3] Present address: 125 Rue du canal, F–57820 Lutzelbourg, France.

* Corresponding author; e-mail Peter.Rogowsky@ens-lyon.fr; fax 334–7272–8607.

Article, publication date, and citation information can be found at http://www.plantphysiol.org/cgi/doi/10.1104/pp.103.030767.

and Gallie, 2000). From a genetic point of view, the embryo and the endosperm have the same gene content but differ in gene dosage. They receive the same haploid parental genomes during fertilization. However, the endosperm receives two copies of the maternal genome and is triploid, contrary to the diploid embryo. Gene expression is often similar, and it has been shown that embryo and endosperm share the expression of several genes that are not expressed in other tissues (Aalen et al., 1994). Concerning their metabolism, both are sink tissues that lack photosynthesis and accumulate reserve substances. Major differences exist in the nature of the stored compounds. The mature maize embryo is rich in lipids, whereas maize endosperm essentially consists of starch granules.

In maize, 51 *emb* mutants were isolated by Clark and Sheridan (1991) and classed according to embryo morphology at kernel maturity (Clark and Sheridan, 1991; Sheridan and Clark, 1993). A more detailed phenotypic characterization of nine mutants with early developmental blocks revealed two major classes. The embryos of the first class resemble wild-type embryos arrested at early developmental stages, whereas the embryos of the second class exhibit aberrant morphology never seen during normal development (Heckel et al., 1999). In addition, the importance of radial differentiation for any further development was demonstrated (Elster et al., 2000). Although the mutants stem from an insertional mutagenesis with the transposon *mutator*, only two of the nine mutants show a genetic cosegregation between the *emb* phenotype and a *mutator* insertion (Heckel et al., 1999). We report here a detailed phenotypic analysis and the molecular cloning of *emb8516*, one of the two potentially tagged mutations. The mutant phenotype is quite variable because of a seemingly uncoordinated proliferation of suspensor tissue. Marker gene analysis demonstrated the presence of suspensor and epidermal identities in mutant embryos. The mutant carries a *mutator* insertion in *ZmPRPL35-1* likely coding protein L35 of the plastid ribosome. This insertion actually causes the phenotype because plants with an independent *mutator* insertion in the same gene also exhibited an *emb* phenotype and because the mutant can be complemented with a genomic clone of *ZmPRPL35-1*. Gene *ZmPRPL35-1* is a low-copy gene that is expressed both in the embryo and the endosperm and in all other tissues analyzed. The possible consequences of plastid dysfunction on embryo and endosperm development will be discussed.

RESULTS

emb8516 Phenotype at Kernel Maturity

To assess the mutant phenotype at kernel maturity, *emb8516* and wild-type kernels were cut in half and observed under a binocular (Fig. 1). Although an embryonic cavern of normal size was formed, this cavern was more or less empty. At the position of the embryo, microscopic structures of variable size and shape were observed that probably corresponded to aborted, desiccated embryos. On the other hand, the endosperm was of normal size and showed the typical texture with a vitreous periphery and a flowery center.

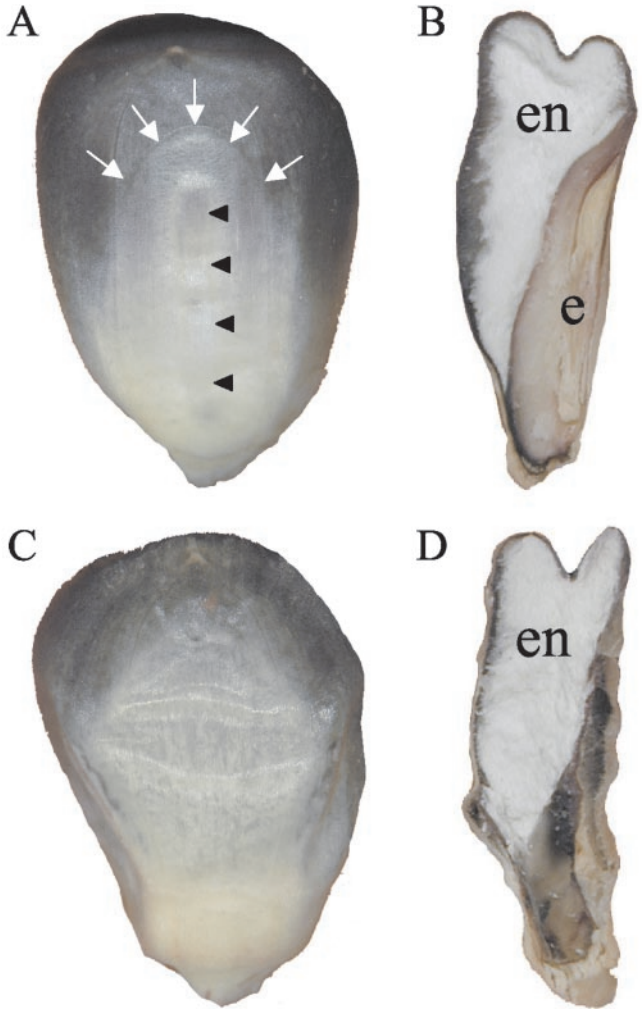

Figure 1. Phenotype of mutant *emb8516* at kernel maturity. Wild-type (A and B) or mutant (C and D) kernels were photographed after harvest and drying. Whole kernels exposing their adaxial side (A and C) or kernels cut in one-half along their longitudinal axis exposing the cut face (B and D) are shown. White arrows point to the imprint of the scutellum, and black arrowheads point to the imprint of the embryo axis. e, Embryo; en, endosperm.

To further characterize the mutant kernels, the major reserve substances were quantified by biochemical methods (Table I). As expected, the amount of fatty acids and ash was drastically reduced in *emb8516* kernels because the embryo was known to be their major storage compartment. In contrast, the amount of starch and protein that are mainly stored in the endosperm was close to that of wild-type kernels, and the small differences could readily be

Table I. *Biochemical analysis of emb8516 and wild-type kernels*

Substance	Wild type[a]	*emb8516*[a]
Starch	678.4	626.0
Fatty acids	63.6	18.0
Amino acids	103.3	80.7
Ash	16.3	10.1

[a] Normalized values in grams per kilogram dry matter.

explained by the fact that small amounts of starch and protein were also stored in the embryo. Predictions made by near-infrared spectroscopy extended the study to over 60 parameters (data not shown) and confirmed our conclusion that the mutation did not seem to have major consequences on endosperm texture or the accumulation of reserve substances in the endosperm.

Variability of the *emb8516* Phenotype

A preliminary description of the *emb8516* phenotype had suggested an aberrant proliferation of suspensor tissue (Heckel et al., 1999). These observations were confirmed and extended by the present study, which was based on confocal microscopy of over 100 dissected mutant embryos from eight sibling plants at three developmental stages (Fig. 2). Strong morphological variations were observed between sister plants and even between mutant kernels stemming from the same ear. At 9 DAP, mutant embryos were less than one-half as long as wild-type siblings and lacked shoot apical meristem, coleoptile, and scutellum (Fig. 2, A–E). Although the overall morphology very much resembled that of wild-type embryos at younger stages (5–7 DAP), some embryos showed aberrations such as a thickening of the embryo (Fig.

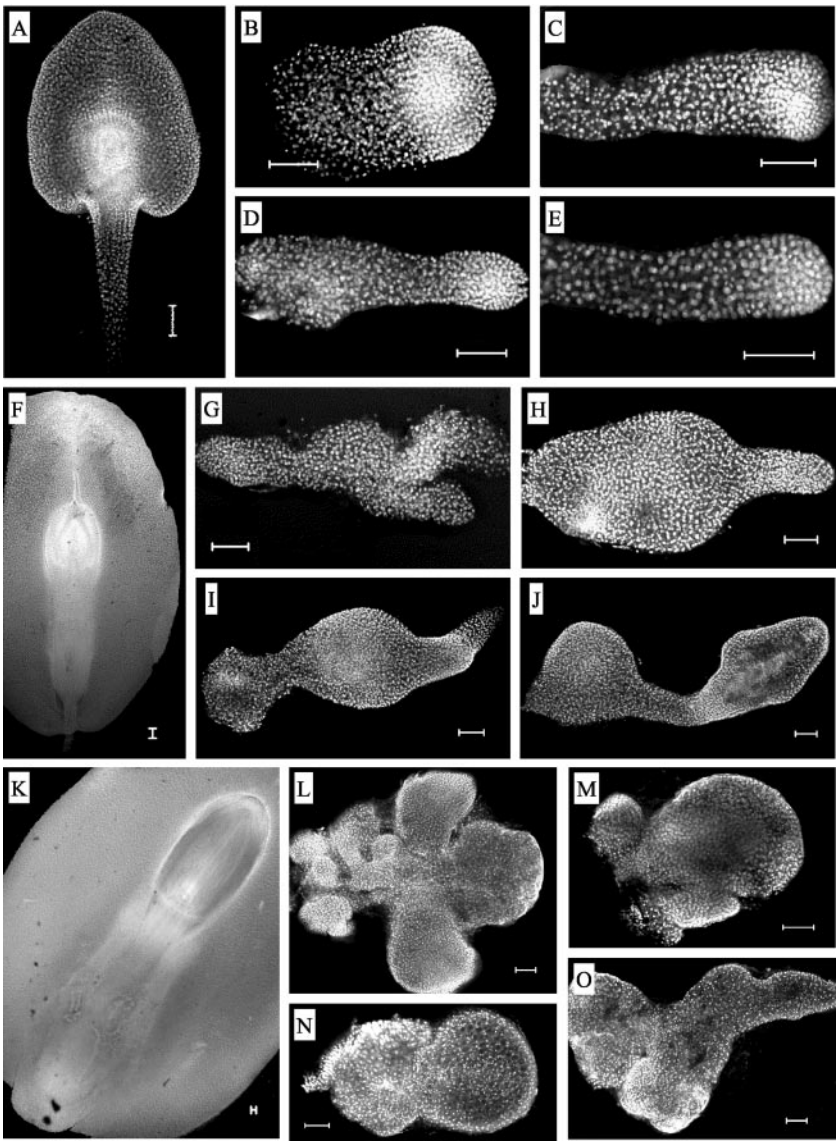

Figure 2. Variable morphology of mutant embryos. Wild-type (A, F, and K) or mutant (B–E, G–J, and L–O) embryos of self-pollinated heterozygous (+/*emb8516*) plants were observed in the confocal microscope at 9 (A–E), 16 (F–J), or 28 (K–O) days after pollination (DAP). The suspensor-like parts of the mutant embryos are always situated at the left side of the photographs. Scale bars = 100 μm.

2B) or small protuberances at the base of the suspensor (Fig. 2D). At 16 DAP, the size differences compared with wild-type embryos were more pronounced, and the typical embryonic structures were still missing (Fig. 2, F–J). The morphological variability among mutant embryos increased and could be resumed by one (Fig. 2, H and J) or two (Fig. 2, G and I) bulbous thickenings of the suspensor-like end and one (Fig. 2, H and J) or two (Fig. 2, G and I) rod-like structures at the embryo proper-like end. At 28 DAP, the majority of mutant embryos had completely lost any resemblance to wild-type embryos of any stage (Fig. 2, K–O). Some had a rather complex morphology (Fig. 2, L and O), whereas others displayed shapes already seen at younger stages (Fig. 2, M and N). Among the protuberances, the smaller ones displayed a much higher density of nuclei, which were generally even more concentrated in the outer cell layers. In summary, the development of mutant embryos deviated before 9 DAP from that of wild-type siblings, leading to callus-like structures of irregular shape and variable size characterized by protuberances at the suspensor-like end.

Expression of Epidermis and Suspensor Marker Genes in *emb8516*

The microscopic observations had suggested the presence of an apico-basal pattern in *emb8516* embryos. To confirm the suspensor identity of the larger cells at the micropylar end and of their outgrowths and to assess radial differentiation and meristem formation, the expression of appropriate marker genes was assayed: *OCL3* for suspensor identity (Ingram et al., 2000), *LTP2* for epidermal cell fate (Sossountzov et al., 1991), and *Kn1* for meristem formation (Smith et al., 1995). In addition, *Esr2* was surveyed, a marker for the embryo-surrounding region (Opsahl-Ferstad et al., 1997), which is linked to the suspensor by plasmodesmata at very early stages (Van Lammeren, 1987). By in situ hybridization of mutant embryos, expression was observed for *OCL3*, *LTP2*, and *Esr2* but not for *Kn1* (Fig. 3). *OCL3* was expressed in the suspensor of wild-type embryos (Fig. 3A). In mutant embryos, the signal extended to various degrees from the suspensor-like part to the more distal parts, generally without reaching the very tip of the embryo (Fig. 3B). In addition, *OCL3* expression was limited to the adaxial side, implying a suspensor identity for this part of the structures observed. Although in wild-type controls *LTP2* expression was restricted to the protoderm at the abaxial side of the embryo proper (Fig. 3C), the signal in mutant embryos extended somewhat to the adaxial side and to the outer cell layer of protuberances from the embryo (Fig. 3D). In the example shown, it covered the entire length of the embryo, possibly indicating an embryo proper identity of the entire abaxial part of the structure observed. Although normal *Kn1* expression was detected in the meristematic zone of wild-type embryos (Fig. 3E), no signal was detected in mutant embryos (Fig. 3F). The expression pattern of *Esr2* marking a specialized zone of the endosperm in the vicinity of the embryo showed no difference between wild-type (Fig. 3G) and mutant endosperm (Fig. 3H). These data clearly demonstrated the epidermal and suspensor fate of certain cells. However, the expression patterns of the respective marker genes were altered, possibly indicating a suspensor/embryo proper

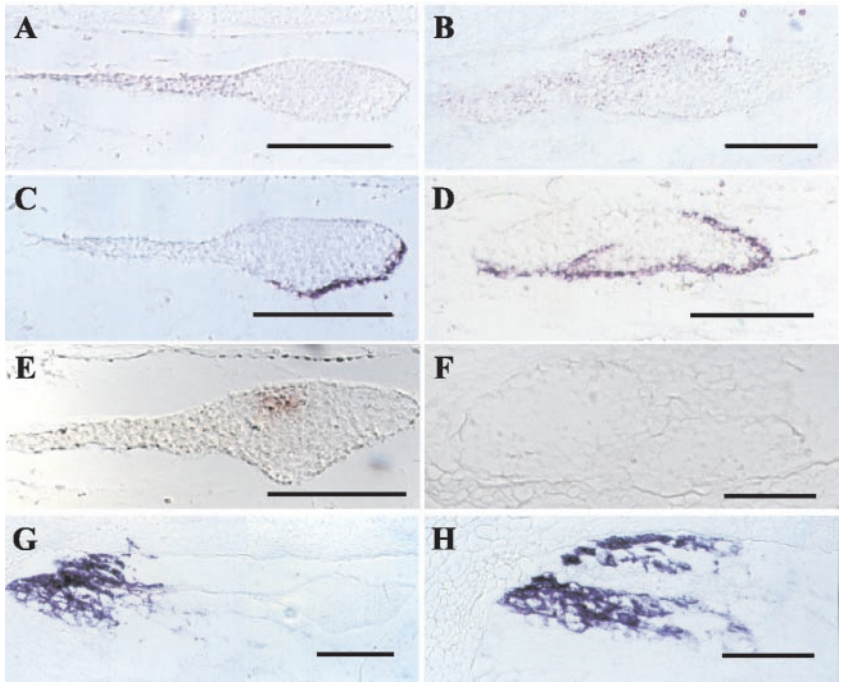

Figure 3. Expression of marker genes in mutant embryos. Wild-type (A, C, E, and G) or mutant (B, D, F, and H) embryos of self-pollinated heterozygous (+/*emb8516*) plants were fixed at 9 (wild type) or 16 (mutant) DAP and imbedded in paraffin. Sections were hybridized in situ with digoxigenin-labeled probes for *OCL3* (A and B), *LTP2* (C and D), *Kn1* (E and F), or *Esr2* (G and H). The suspensor-like parts of the mutant embryos are always situated at the left in the photographs. Scale bars = 50 μm.

boundary oblique rather than perpendicular to the apical-basal axis.

Cloning of a *mutator* Insertion Cosegregating with the *emb8516* Phenotype

The mutation *emb8516* had been isolated in a population mutagenized with the transposon *mutator* and cosegregation of a particular *mutator* insertion with the *emb* phenotype had been observed with the amplification of insertion mutagenized sites (AIMS) technique (Heckel et al., 1999). We now cloned and sequenced the 107-bp AIMS fragment (AIMS in Fig. 4A). It contained 70 bp of flanking region, which was extended by bidirectional genomic walk on wild-type DNA (GW1-3 and GW1-4 in Fig. 4A). Partial similarity to maize cDNA clone MEST6-D3 (GenBank accession nos. AI001298 and AI374506) suggested that the insertion in *emb8516* was located in an intron of the gene corresponding to MEST6-D3. A complete genomic clone covering the entire region (LC1-13 in Fig. 4A) was eventually obtained by the screen of a genomic library. Ab initio annotation of its sequence with the program Genscan (http://genes.mit.edu/GENSCAN.html) predicted a single open reading frame (ORF) composed of three exons that were all present on MEST6-D3. The entire predicted ORF was amplified by reverse transcriptase (RT)-PCR on young leaf cDNA, and its sequence was shown to be 99% similar to MEST6-D3. Comparison with the genomic sequence revealed two introns with canonical splice sites.

To determine the copy number in the maize genome, the full-length cDNA sequence present on MEST6-D3 was used as a probe on genomic DNA gel blots. Under moderate stringency, between one and two major bands were observed indicative of a single- or low-copy gene (Fig. 4B).

Sequence Analysis of *ZmPRPL35-1*

The amino acid sequence of the gene disrupted by the *mutator* insertion in *emb8516* showed high similarity to protein L35 that was part of 50S ribosomes in plastids. The gene was consequently called *ZmPRPL35-1*. In Figure 5, the position of the Prosite signature for L35 proteins was indicated and the Pfam consensus sequence aligned with ZmPRPL35-1. The sequence analysis hereafter is based on the spliced genomic sequence of clone LC1-13 because this clone was obtained without PCR, and its sequence was not likely to reflect errors of the *Taq* polymerase.

In the amino acid sequence of ZmPRPL35-1, a signal peptide was predicted by the program SignalP (http://www.cbs.dtu.dk/services/signalP/Peptide Signal). A plastid score of 0.971 was obtained with the program Predotar (http://genoplante-info.infobiogene.fr/predotar.html). Both results were consistent with previous reports suggesting that L35 proteins were encoded in the nucleus of higher plants, whereas they were located in the plastid in algae and lower plants (Smooker et al., 1990). N-terminal sequencing had shown that in spinach, the mature protein was similar in size to the primary translation product of unicellular organisms such as *P. purpurea* or *C. paradoxa* (Fig. 5). Interestingly, the similarity of ZmPRPL35-1 with the other known higher plant L35 proteins in spinach (GenBank accession no. AAA34043) and Arabidopsis (GenBank accession no. CAA60774) was restricted to the region of the mature spinach protein (Fig. 5).

A BLAST search with *ZmPRPL35-1* in the GenBank dbest database revealed the existence of additional putative L35 genes in higher plants (wheat [*Triticum aestivum*], barley [*Hordeum vulgare*], rice [*Oryza sativa*], potato [*Solanum tuberosum*], tomato [*Lycopersicon esculentum*], and soybean [*Glycine max*]) and the moss *P. patens*. In all species, at least one EST with an N-terminal extension beyond the mature spinach protein was found. Consensus sequences were established and aligned (Fig. 5). In general, the putative mature proteins were highly conserved, whereas the putative signal peptides were quite divergent. Nevertheless, three regions marked by blue rectangles in Figure 5 were identified in the putative precursor

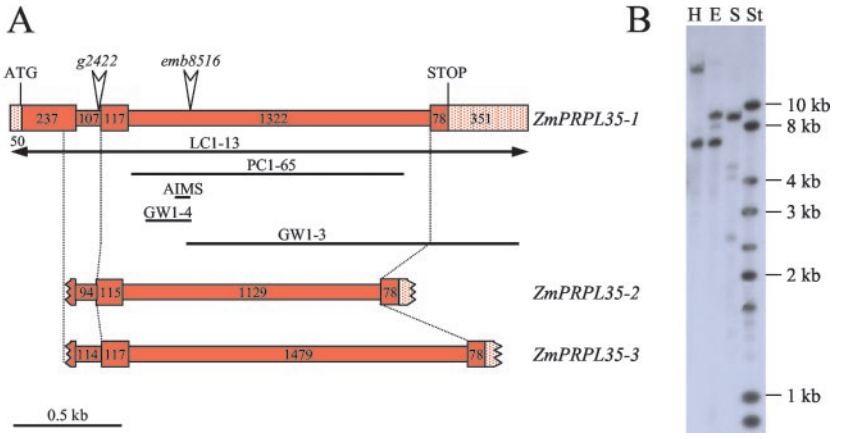

Figure 4. *ZmPRPL35* gene structure. A, In a schematic drawing, the three *ZmPRPL35* genes are depicted to the extent known by sequence analysis. Exons and introns are presented as wide and narrow rectangles, respectively. Numbers indicate their size in base pairs. Horizontal bars below the drawing correspond to genomic clones mentioned in the text that were obtained by library screen (LC), genomic walk (GW), genomic PCR (PC), or AIMS. In the case of the double-headed arrow, only part of the clone was drawn. The insertion sites of *mutator* elements in mutants *emb8516* and *g2422* are represented by vertical arrowheads. B, DNA gel blot of genomic maize DNA with the *ZmPRPL35-1* cDNA probe RT58-1. E, *Eco*RI; H, *Hind*III; S, *Sal*I; St, size standard.

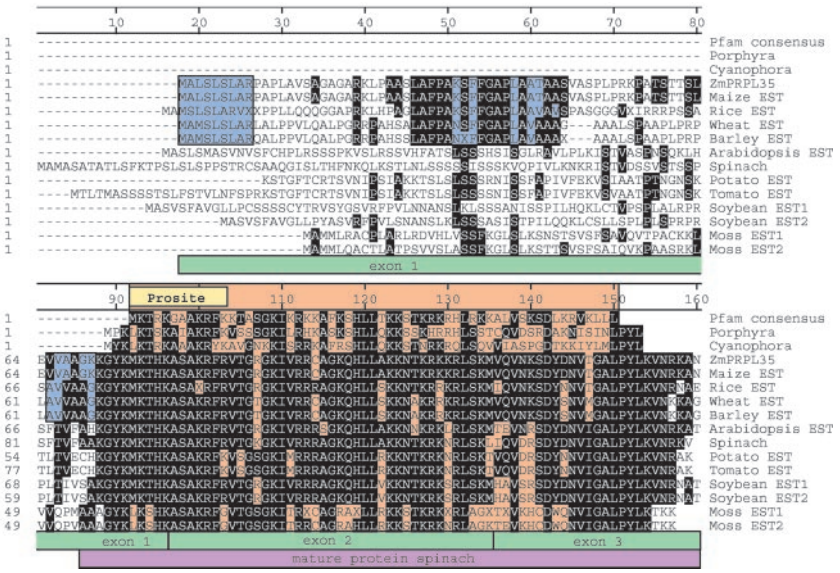

Figure 5. ZmPRPL35 carries the signature of L35 proteins. The amino acid sequence of ZmPRPL35-1 was aligned with the PRPL35 consensus sequence of the Pfam database; the sequences of the known PRPL35 proteins from *Porphyra purpurea*, *Cyanophora paradoxa*, and spinach (*Spinacia oleracea*); and with amino acid sequences deduced from expressed sequence tag (EST) consensus sequences (see "Materials and Methods") of *Physcomitrella patens* and several higher plants. The position of the Pfam RPL35 consensus sequence, the Prosite RPL35 signature, and the mature spinach protein are shown by red, yellow, and purple rectangles, respectively. Blue rectangles, regions of high similarity between cereal sequences; green rectangles, intron/exon boundaries of ZmPRPL35.

parts that were conserved within the clade of monocotyledonous plants but not between monocotyledonous and dicotyledonous plants.

In maize, a total of 33 ESTs covering the entire Pfam consensus were assembled into the consensus sequence "maize EST," which was identical to the predicted amino acid sequence of ZmPRPL35-1. The junctions between signal peptide, preprotein, and mature protein did not coincide with the intron/exon splice junctions. Take together, all these data suggested that the gene disrupted in *emb8516* was a structural component of the plastid ribosome.

Isolation of an Independent *mutator* Insertion in *ZmPRPL35-1*

To prove that the *mutator* insertion in *ZmPRPL35-1* actually caused the *emb* phenotype of mutant *emb8516*, a second allele was isolated by a reverse genetics approach. A PCR screen of 25,000 plants carrying a high number of *mutator* insertions revealed a single plant with a germinal insertion. In plant G2422, a *mutator* element was inserted in intron 1 of *ZmPRPL35-1* just 3 bp upstream of the junction between intron 1 and exon 2 (Fig. 4A).

To test the allelic relationship between mutations *emb8516* and *g2422*, 15 heterozygous plants *+/emb8516* were pollinated by six heterozygous plants *+/g2422*. In all cases, approximately one-quarter of the kernels on the cross-pollinated ears had an *emb* phenotype (Exp. I in Table II). Siblings of the plants used for the allelism test were crossed to inbred line A188 and stock Rscm2. The offspring was used for two further complementation experiments involving reciprocal crosses in an A188 background (Exp. II in Table II) and an Rscm2 background (Exp III in Table II). The ratio of *emb* kernels in crosses between the two mutants *emb8516* and *g2422* (between 16% and 20%) was very similar to the one observed in self-pollinations of either mutant (16%–23%). These data confirmed that mutant *g2422* did not complement mutant *emb8516* and, therefore, carried a lesion in the gene responsible for the *emb8516* phenotype.

The phenotype of mutant *g2422* was assessed in self-pollinated siblings of the plants used for the allelism tests II and III. All ears harvested from plants carrying the *mutator* insertion in intron 1 exhibited approximately one quarter of kernels with an *emb* phenotype (Table II). Taken together, these data strongly supported the hypothesis that insertions in *ZmPRPL35-1* caused an *emb* phenotype.

Complementation of *emb8516* by a *ZmPRPL35-1* Transgene

Irrevocable proof that the *mutator* insertion in *ZmPRPL35-1* actually caused the *emb* phenotype of mutant *emb8516* was obtained by the complementation of the mutant with a genomic clone of *ZmPRPL35-1*. The 5.8-kb insert of clone LC1-13 (Fig. 4) containing 2.05 kb upstream and 1.90 kb downstream sequence was cloned in a vector allowing maize transformation via *Agrobacterium tumefaciens*. Primary transformants corresponding to 17 independent transformation events were pollinated by heterozygous *+/emb8516* plants. T_1 plantlets carrying the transgene were genotyped for the presence or absence of the *emb8516* mutation and self-pollinated. For each transformation event, the ears of at least two *+/emb8516* T_1 plants and one *+/+* plant were scored. In the 16 of 17 cases, the average value of *emb* kernels on ears of *+/emb8516* plants was close to the 6.25% expected in the case of complementation with an average value of 5.64% over the 16 events (Table III). In one case, the average value was 17.2%, which

Table II. *Frequency of emb phenotype after crosses and self-pollinations involving mutants emb8516 and g2422*

Female	Male	Exp[a]	No. of Pollinations	No. of Ears with *emb* Phenotype[b]	*emb* Kernels per Ear	SE	*emb* Kernels per Ear
					%		%
+/emb8516	+/g2422	I	15	15	23.6	±7.9	21
		II	4	4	19.0	±1.6	
		III	11	11	20.2	±2.1	
+/g2422	+/emb8516	I	nd	nd	nd	nd	19
		II	7	7	16.4	±7.4	
		III	9	9	21.1	±3.7	
+/+	+/g2422	I	nd	nd	nd	nd	1
		II	5	0	0.7	±1.4	
		III	5	0	1.2	±1.4	
+/+	+/emb8516	I	nd	nd	nd	nd	1
		II	5	0	1.4	±1.3	
		III	6	0	0.8	±1.3	
+/g2422	+/g2422	I	nd	nd	nd	nd	19
		II	11	11	16.4	±9.8	
		III	10	10	20.8	±3.8	
+/emb8516	+/emb8516	I	11	11	25.0	±7.0	23
		II	8	8	20.8	±3.4	
		III	14	14	22.6	±2.7	

[a] Three experiments (I–III) were performed on subsequent generations. [b] Only ears above the background value of 2% *emb* kernels were counted.

was closer to the 25% expected in the case of noncomplementation, especially because the actual values observed on ears of self-pollinated mutants rarely surpass 20% (Table III). This case was interpreted as a transformation event with poor transgene expression, possibly because of the insertion site in the genome. Finally, on the ears of the +/+ control plants, the ratio of *emb* kernels never surpassed 0.6% (Table III). Taken together, these data clearly demonstrated the complementation of the *emb8516* mutation by *ZmPRPL35-1*.

Mapping and Copy Number of *ZmPRPL35*

RFLP mapping of a *ZmPRPL35-1* cDNA clone on a Limagrain mapping population revealed two distinct positions in Bin 6.02 on chromosome arm 6L and in Bin 9.03 on chromosome arm 9L. The two map positions were not part of the chromosomal regions sharing extensive similarity and reported as being involved in genome duplications in maize (Helentjaris, 1995). To assign *ZmPRPL35-1* to one of the two possible positions, an intron probe (PC1-65 in Fig. 4) was mapped on the Brookhaven National Laboratory (Upton, NY) inbred mapping population CO159 × TX303. The only exploitable polymorphism was located in Bin 9.03. Because it corresponded to the strongest band, *ZmPRPL35-1* likely mapped to 9L rather than 6L.

Both the genomic Southern blot (Fig. 4B) and the mapping had indicated the existence of one or two genes related to *ZmPRPL35-1*. During our diverse cloning efforts, two additional genomic DNA fragments related but not identical to *ZmPRPL35-1* had been isolated and named *ZmPRPL35-2* and *ZmPRPL35-3* (Fig. 4A) They diverged considerably from *ZmPRPL35-1* both in the length and sequence of the two introns, showing only 71% and 93% similarity, respectively. On the other hand, the exon sequences were highly conserved with 95% and 99% similarity, respectively. However, only *ZmPRPL35-3* potentially coded for a protein comparable with ZmPRPL35-1 because in the case of *ZmPRPL35-2*, a 2-bp deletion in exon 2 disrupted the ORF. Either

Table III. *Complementation of emb8516 with a ZmPRPL35-1 transgene*

Genotype Mutation	Genotype Transgene	No. of Transformation Events	No. of Ears Scored	No. of Ears with *emb* Phenotype	*emb* Kernels per Ear[a]	SE
					%	
+/emb8516	Hemizygous	16	46	46	5.7%	±2.3
		1	3	3	17.2%	±3.9
+/+	Hemizygous	17	17	0	0.1%	±0.1
+/emb8516	Absent	–	8[b]	8[b]	20.8[b]	±3.4[b]

[a] Theoretical nos. are 6.25% (complementation) or 25% (absence of complementation). [b] Taken from Table II.

ZmPRPL35-2 or *ZmPRPL35-3* may be located at the second mapping position obtained with a cDNA probe of *ZmPRPL35-1*.

Constitutive Expression of *ZmPRPL35-1*

One possible explanation for the embryo-specific phenotype of insertions in *ZmPRPL35-1* was a differential gene expression between embryo and endosperm. Therefore, the expression of *ZmPRPL35* was compared with that of the *Gapdh* by semiquantitative RT-PCR not only in different maize tissues (Fig. 6, A and B) and during kernel development (Fig. 6, C and D) but also in microdissected wild-type and mutant embryos and endosperms (Fig. 6, E and F). *ZmPRPL35* expression at various levels was detected in all tissues examined. It was highest in young leaves, the tissue with the highest photosynthetic activity. Low expression was observed in non-photosynthetic tissues such as roots or kernels. Most importantly, expression was diminished more than 10-fold in both the embryo and endosperm of mutant *emb8516* as compared with wild-type controls.

The high similarity between the ORFs of the three known *ZmPRPL35* genes and the absence of sequence data in the 3′-untranslated region of *ZmPRPL35-2* or *ZmPRPL35-3* made it impossible to design gene-specific primers. The primers chosen allowed the detection of all three genes (*ZmPRPL35-1*, *ZmPRPL35-2*, and *ZmPRPL35-3*). The strong diminution of expression in mutant embryos and endosperms suggested that at least in these tissues, the detected single band of 489 bp reflected largely if not exclusively the expression of *ZmPRPL35-1*.

This was further confirmed by cleaved-amplified polymorphic sequence experiments exploiting single nucleotide polymorphisms (SNPs) between the three genes (Fig. 7A). RT-PCR products obtained with primers in identical regions were not cut by *Ava*II or *Bsp*MI, indicating that neither *ZmPRPL35-2* nor *ZmPRPL35-3* were expressed in the tissues tested (Fig. 7B). Restriction with *Taq*I and absence of restriction with *Bsp*MI showed that only *ZmPRPL35-1* was expressed in wild-type and mutant embryo and endosperm and in light-grown seedlings.

Functional Plastids in *emb8516*

Because several pathways in the primary metabolism of plant cells take place at least partially in plastids, the embryo lethal phenotype of mutant *emb8516* could be readily explained by the disruption of these pathways because of impaired translation in the absence of protein L35. To test this hypothesis, the ultrastructure of wild-type and mutant embryos from the same ear was compared at 20 DAP. The analysis of a mutant with enlarged suspensor of the type depicted in Figure 5H is resumed in Figure 8. Light microscopical analysis of thin sections showed that the cells in this mutant embryo did not resemble the three major cell types found in the apical part of wild-type embryos, i.e. in scutellum, coleoptile, or leaf primordia (Fig. 8, A and B). Electron microscopy of adjacent ultrathin sections confirmed that neither the small cells rich in cytoplasm of the embryo axis (Fig. 8C) nor the large vacuolized cells of the scutellum (Fig. 8D) were found in the mutant. Mutant cells exhibited typical signs of necrosis such as leakage of cytoplasm into vacuoles. They were completely disorganized, and it was nearly impossible to identify their different components (Fig. 8E). Electron dense bodies at organelle boundaries (arrowheads in Fig. 8E) possibly corresponded to membrane agglomerates. On the contrary, typical signs of programmed cell death such as vacuolar dilatations or nuclear fragmentation were not observed (Dominguez et al.,

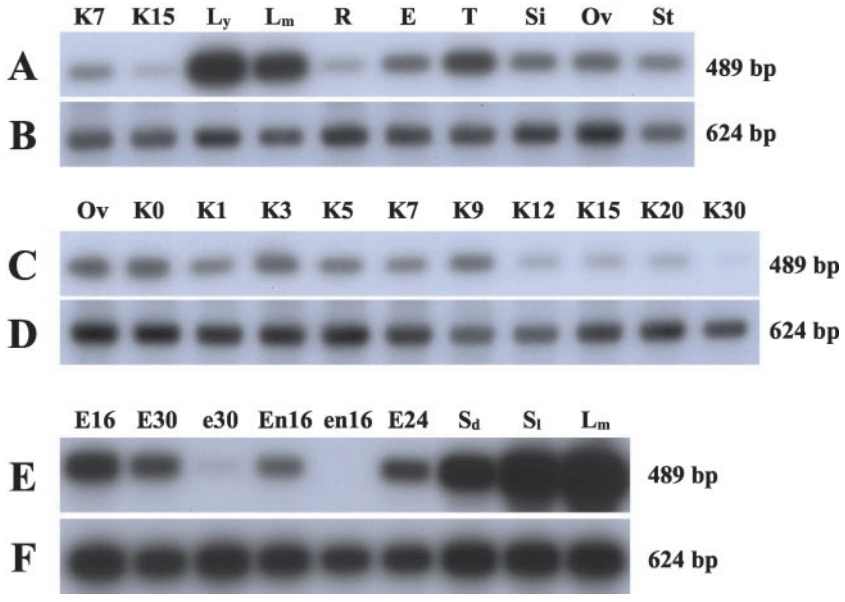

Figure 6. *ZmPRPL35* expression in wild-type and mutant tissues. Expression of *ZmPRPL35* (A, C, and E) and a *Gapdh* control (B, D, and F) in various tissues of the maize plant (A and B), at various stages of kernel development (C and D), and in mutant and wild-type tissues (E and F) was monitored by RT-PCR. Equal amounts of total RNA were used for the reactions. PCR products were separated by gel electrophoresis, blotted onto nylon membranes, hybridized with a *ZmPRPL35* probe, and detected by autoradiography. E, Immature ear; E16, wild-type embryo at 16 DAP; E24, wild-type embryo at 24 DAP; E30, wild-type embryo at 30 DAP; e30, mutant embryo at 30 DAP; En16, wild-type endosperm at 16 DAP; en16, mutant endosperm at 16 DAP; KX, kernel at X DAP; L_m, mature leaf; L_y, young leaf; Ov, ovule; R, root; S_d, dark-grown seedling; Si, silk; S_l, light-grown seedling; St, stem; T, tassel.

2001). The presence of starch grains in structures surrounded by double membranes allowed their identification as plastids both in wild type and the mutant (Fig. 8, F and G). Therefore, at least all the mechanisms necessary for starch synthesis and accumulation were functional in the mutant, arguing against a major and general disruption of plastid function.

DISCUSSION

Here, we present evidence that a *mutator* element cosegregating with the *emb8516* mutation is inserted in a gene that was called *ZmPRPL35-1* because of the presence of a well-established signature for protein L35 of the large subunit of plastid ribosomes. The isolation of a second allele *g2422* carrying an independent *mutator* insertion in the same gene and the complementation of the *emb8516* mutation by a *ZmPRPL35-1* transgene confirm our hypothesis that correct expression of *ZmPRPL35-1* is needed for normal embryo development beyond the transition stage. In contrast, disruption of *ZmPRPL35-1* does not affect the parallel development of the endosperm, which is the second product of the double fertilization and shares with the embryo the same genetic constitution and a heterotrophic metabolism. As a consequence, proper embryo development may depend to a much larger degree on functional plastids than endosperm development. Alternatively, ZmPRPL35-1 may have other roles than just that of a structural protein contributing to the functioning of the plastid translational machinery.

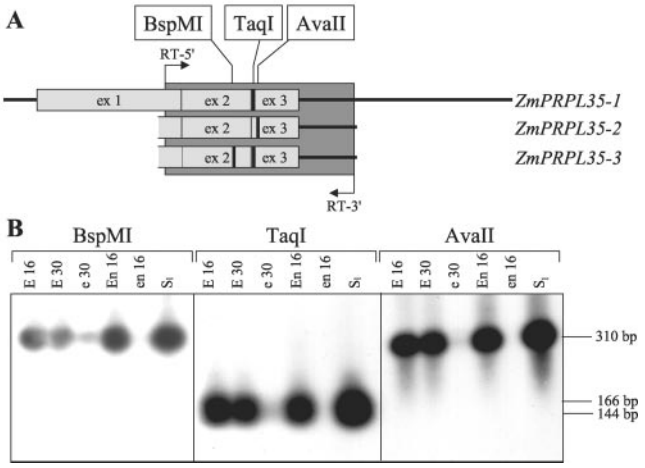

Figure 7. Absence of expression of *ZmPRPL35-2* and *ZmPRPL35-3*. The primers RT-5′ and RT-3′ situated in identical regions of *ZmPRPL35-1*, *ZmPRPL35-2*, and *ZmPRPL35-3* were used to amplify cDNA of six different tissues. RT-PCR products were digested with restriction enzymes recognizing SNPs between the three *ZmPRPL35* genes before gel electrophoresis. A, Schematic drawing indicating the amplified region in dark gray and the presence of restriction sites by fat vertical bars. The gene structure is indicated by horizontal bars (5′- and 3′-untranslated region) and light-gray boxes (exons). Only the parts with available sequence information of the three *PRPL35* genes are shown. B, Autoradiograph of the agarose gel hybridized with the *ZmPRPL35-1* cDNA probe RT58-1. The autoradiographs were voluntarily overexposed to visualize traces of digested or nondigested DNA. E16, Wild-type embryo at 16 DAP; E30, wild-type embryo at 30 DAP; e30, mutant embryo at 30 DAP; En16, wild-type endosperm at 16 DAP; en16, mutant endosperm at 16 DAP; S_l, light-grown seedling.

Aberrant Suspensor Morphogenesis

Our phenotypic analysis of *emb8516* embryos employed confocal microscopy to assess embryo morphology and in situ hybridization to follow marker gene expression. Despite a certain phenotypic variability, all *emb8516* embryos undergo at least partial pattern formation. All mutant embryos acquire an apico-basal pattern as seen by a rod-like rather than spherical overall shape and by different cell types at the suspensor-like and embryo proper-like end. In most cases, the inside-outside pattern is established at least in some parts of the embryo, as demonstrated by expression of the *LTP2* marker gene. Therefore, radial differentiation is uncoupled from morphogenesis as previously shown in Arabidopsis *raspberry* embryos (Yadegari et al., 1994). On the contrary, the absence of expression of the *Kn1* marker gene in in situ hybridizations suggests that no functional meristems are formed.

Contrary to pattern formation, morphogenesis is completely aberrant. Already at 9 DAP, mutant embryos are considerably smaller than wild-type siblings, and at least some of them show a thickening of all or part of the suspensor-like end. None of the mutant embryos display the typical triangular shape of the scutellum or the circular shape of the coleoptile. At later stages, the simplest interpretation of the observed structures is a non-coordinated, irregular proliferation of suspensor-like tissue and the absence of morphogenesis in the embryo proper-like part. Similar phenotypes have been observed in the large and heterogeneous groups of *raspberry* and *suspensor* mutants in Arabidopsis and have been explained by aberrant signaling events between the suspensor and the embryo proper (Schwartz et al., 1994; Yadegari et al., 1994). The parallel goes even further in the case of the *rsy3*. Not only do *rsy3* embryos show a suspensor thickening very similar to that of *emb8516* embryos, but both underlying genes code for plastidial proteins (Apuya et al., 2002). In light of three other examples where embryo development is altered at early stages because of lesions in plastid-targeted proteins, our study provides additional support to the conclusion of Apuya et al. (2002) that functioning of these genes is a prerequisite for the synthesis of embryo signaling molecules.

At 28 DAP, some mutant embryos reached almost one-quarter of the size of wild-type siblings, indicating that the basic steps of cell division and cell growth were probably not severely affected. The

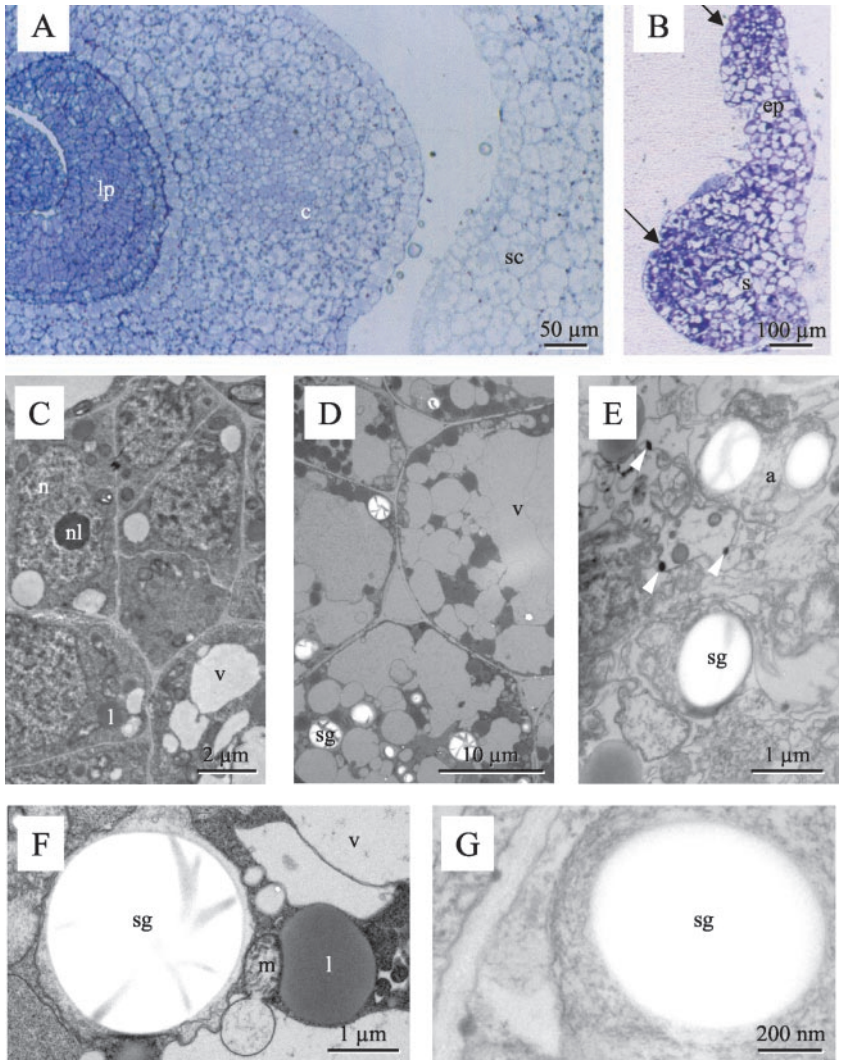

Figure 8. Ultrastructure of mutant embryos. Wild-type embryos (A, C, D, and F) or embryos of mutant *emb8516* (B, E, and G) were fixed, sectioned, stained, and observed in the light (A and B) or electron microscope (C–G). A, Transverse section showing different cell types in the scutellum (sc), coleoptile (c), and leaf primordia (lp). B, Longitudinal section depicting embryo proper-like (ep) and suspensor-like (s) structures. Arrows indicate two regions of smaller cells. C, Small cells rich in cytoplasm typical of the embryo axis. D, Highly vacuolized cells of the scutellum. E, Disorganized mutant cells. Arrowheads point at electron dense material possibly corresponding to aggregated membranes. F and G, Amyloplasts with starch grains. a, Amyloplast; c, coleoptile; ep, embryo proper; l, liposome; lp, leaf primordium; m, mitochondrium; n, nucleus; nl, nucleolus; s, suspensor; sc, scutellum; sg, starch grain; v, vacuole.

leakage of cytoplasm into vacuoles and the absence of nuclear fragmentation suggest that the mutant embryos undergo necrosis rather than programmed cell death. At maturity, only microscopic structures were present in the kernel, possibly because mutant embryos do not resist the dehydration process. Biochemical quantification of reserve substances and near-infrared spectroscopy at kernel maturity revealed statistically significant differences only for embryo-related traits such as fatty acid content but not for numerous tested endosperm-related traits such as starch content and composition.

Structure of the *ZmPRPL35* Gene Transferred from Plastids to the Nucleus during Evolution

The amino acid sequence of the gene disrupted by the *mutator* insertion in *emb8516* carried the signature of L35 proteins that are part of 50S ribosomes in plastids. As a consequence, the gene was called *ZmPRPL35-1*. In higher plants, about 60% of the plastidial ribosomal proteins (PRPs) are encoded in the nucleus (Yamaguchi and Subramanian, 2000; Yamaguchi et al., 2000). During their transfer from the plastid to the nuclear genome, two major changes occurred during evolution: the acquisition of transit peptides and the appearance of introns. These events do not seem to be related in the case of ZmPRPL35-1, where exon 1 contains both the putative transit peptide and part of the Prosite signature for PRPL35. With 71 amino acids, the size of the transit peptide is unusually long compared with the average of all types of proteins. However, relatively long transit peptides seem to be a general rule for small mature peptides and may play a role in the proper import and processing of small basic proteins in the plastids (Yamaguchi and Subramanian, 2000).

The homologies to intron-less L35 proteins from bacteria and lower eukaryotes extend from exon 1 over exon 2 into exon 3. This distribution of intron/exon boundaries is not unique to maize but conserved in Arabidopsis and rice, the two other higher plants where both genomic and EST sequence data are available (Fig. 5; GenBank accession nos.

AC005170 and AP003517). However, intron sizes differ greatly between Arabidopsis (350–633 bp) on one hand and the cereals rice (83–1,276 bp) and maize (107–1,322 bp) on the other.

Although only one *PRPL35* gene is present in the Arabidopsis and rice genomes, we isolated two partial genomic clones in addition to *ZmPRPL35-1*. *ZmPRPL35-2* carries a 2-bp deletion in exon 2 and does not code for a functional protein. Conversely, the partial sequence of ZmPRPL35-3 is 99% similar to ZmPRPL35-1 in the sequenced region, which corresponds to the strongly conserved part of the protein and excludes the more variable signal peptide.

Two distinct map positions for *ZmPRPL35* genes were identified in the maize genome. They were not part of the chromosomal regions sharing extensive similarity and reported as being involved in genome duplications in maize (Helentjaris, 1995). The most likely position for *ZmPRPL35-1* is on chromosome 9 in a region showing synteny to the part of rice chromosome 6 where the single rice ortholog is located.

Expression of *ZmPRPL35*

Only *ZmPRPL35-1* is expressed among the three *ZmPRPL35* genes as shown by cleaved-amplified polymorphic sequence experiments exploiting SNPs between the three genes. This result is in agreement with in silico analysis of EST abundance: 47 of the 48 ESTs in GenBank fully match *ZmPRPL35-1* at the positions of the three SNPs distinguishing *ZmPRPL35-1* from *ZmPRPL35-3*, whereas one EST from cold-stressed seedlings is more similar to *ZmPRPL35-3* (two of three SNPs) than to *ZmPRPL35-1* (one of three SNPs). Because of the high level of polymorphisms between maize genotypes and the possibility of sequence errors in ESTs, it remains difficult to draw a definite conclusion as to a possible low level expression of *ZmPRPL35-3* in certain tissues or under certain conditions. Our experimental data clearly indicate that this expression was below the detection level in the tissues tested, which include embryo and endosperm, possibly because of mutations in the non-sequenced 5′ end of the gene. Not surprisingly, there is no EST reflecting the nonfunctional gene *ZmPRPL35-2*.

As expected for a gene encoding a structural protein present in plastids, *ZmPRPL35-1* is expressed throughout the plant in green and non-green tissues with highest expression in young leaves. During kernel development, expression declines gradually in the maturation phase. The gene is transcribed both in the embryo and the endosperm, and transcription is strongly decreased both in homozygous mutant embryos and endosperms of *+/emb8516* plants.

Therefore, the embryo-specific phenotype of mutant *emb8516* cannot be explained by differential gene expression between embryo and endosperm of any of the three *ZmPRPL35* genes. Although we cannot formally exclude the existence of an additional *ZmPRPL35* gene, the existence of such a gene is not very likely in light of all the data concerning gene copy number in maize and other species. In addition, this gene would have to be expressed in the endosperm but not in the embryo.

The Role of Plastids in Embryo and Endosperm Development

It is generally admitted that plastids play a fundamental role in the basic metabolism of plant cells; for example, several steps of the fatty acid synthesis occur in this organelle. In addition, important steps in the biosynthesis of plant hormones such as GA or abscisic acid take place in plastids. These steps occur not only in chloroplasts but also non-specialized proplastids and other types of plastids (Taiz and Zeiger, 1998). Therefore, it is not surprising that defects in the plastid translational machinery could have affects on all types of tissues, including embryo and endosperm. Embryo-lethal phenotypes have been reported in Arabidopsis for mutations in genes coding for components of the translational machinery of plastids (Uwer et al., 1998; Apuya et al., 2001) or for plastid-targeted proteins of unknown function (Albert et al., 1999; Apuya et al., 2002). On the other hand, the published mutants in genes coding for plastid ribosomal proteins are not embryo lethal (Schultes et al., 2000; Pesaresi et al., 2001; Woo et al., 2002; Horiguchi et al., 2003).

Several conclusions can be drawn from these studies. First, not all mutations in plastid ribosomal proteins have the same phenotype. This is consistent with findings in *Escherichia coli* that show that the loss of some ribosomal proteins is not lethal and can be tolerated with more or less severe consequences (Dabbs, 1991). Second, a lower translation rate in plastids does not necessarily lead to an embryo-lethal phenotype. In vivo translation assays show that in the *prpl11-1* mutant, the plastid ribosome activity per se is lowered without any reported effects on embryo development (Pesaresi et al., 2001). Third, the external application of a missing component of the translational machinery does not necessarily compensate the lesion. *edd1* embryos lacking glycyl-tRNA synthetase can only be rescued partially by in vitro culture on nutritive media. According to the authors, this contradicts the hypothesis of a simple metabolic deficiency causing the developmental arrest and indicates that additional mechanisms are probably affected in the mutant (Uwer et al., 1998). Similarly, in the discussion of the *rfc3* mutant impaired in an PRPS6-like gene, an involvement in plastid-nucleus communication is evoked (Horiguchi et al., 2003). Such a more complex explanation may also be appropriate in the case of our mutant *emb8516*.

In fact, it is quite difficult to link the observed mutant phenotype to the absence of a plastid ribo-

somal protein. Considering the fact that PRPL35 does not belong to the essential ribosomal proteins in *E. coli* (Dabbs, 1991), it seems straightforward to postulate that the mutation might cause a slowdown rather than arrest of protein synthesis in plastids and, as a consequence, a metabolic deficiency of embryo cells that ultimately leads to the abortion of the embryo. However, this hypothesis only accounts for part of the phenotype and does not explain the normal development of the endosperm. In addition, one might expect to find morphologically normal embryos arrested at early stages rather than aberrant morphogenesis. One of several possible explanations is based on the observation that embryo and endosperm have completely different developmental fates and, therefore, may have different needs for molecules synthesized in plastids. Variations in the level of plant hormones such as GA or abscisic acid, of auxin precursors, or of developmentally important metabolites such as Suc (Weber et al., 1997) might explain both the embryo and the endosperm phenotype.

MATERIALS AND METHODS

Plant Material

Mutants *emb8516* (Clark and Sheridan, 1991) and *g2422* were maintained as heterozygotes. They were backcrossed to inbred line A188 (Gerdes and Tracy, 1993) and to a genetic stock carrying the *R-scm2* allele responsible for anthocyanin coloration of the scutellum of the embryo (Clark and Sheridan, 1991). To ascertain the presence of the mutation, the pollen donors were self-pollinated and scored for ears with a segregation ratio of 3:1 for wild-type:*emb* phenotype kernels. Inbred line A188 and stock Rscm2 were also used for genomic walk and expression studies, whereas hybrid DH5 × DH7 (Barloy et al., 1989) served for the construction of a genomic library. Plants were generally grown in a green house with a 16-h illumination period (100 W m^{-2}) at 24°C/19°C (day/night). Backcrosses and part of the complementation were performed in the field in Lyon (France).

Allelism Tests

All plants destined for allelism tests were genotyped by PCR to verify the presence of the respective *Mu* insertion. Primers Mu12 (5′ GAATCCCTTCCGCTCTTCGTCTA 3′) and 8516e (5′ ATTGCCTGTTTTAATAGCTGTACATAGAAA 3′) were used for mutant *emb8516* and primers OMuA (5′ CTTCGTCCATAATGGCAATTATCTC 3′) and 2k (5′ CATCTTCGAGAGCCTCTTCTTGCG 3′) for *g2422*. Positive plants were crossed either by a standard technique or by the double-pollination technique described previously (Heckel et al., 1999). The *emb* phenotype of the male was checked by self-pollination and subsequent scoring of the mature ear for the presence of one-quarter *emb* phenotype kernels. Similarly, the *emb* phenotype of the female was ascertained on the self-pollinated one-half of the ear in the case of double pollination. For the cross, the segregation ratio of wild-type:*emb* phenotype kernels was determined at maturity.

DNA Manipulations

If not specified otherwise, all DNA and RNA manipulations were performed according to Sambrook et al. (1989). Plant DNA was isolated from approximately 10 cm^2 of young leaf material. The tissue was ground in an Eppendorf tube (Eppendorf Scientific, Westbury, NY) in the presence of liquid nitrogen, suspended in 500 μL of extraction buffer (100 mM Tris-HCl, 50 mM EDTA, 100 mM NaCl, and 1% [w/v] SDS [pH 8]) and incubated at 65°C for 5 min. After two extractions with equal volumes of phenol/chloroform, the DNA was precipitated in the presence of 0.3 M Na-acetate with 0.6 volumes of ice-cold isopropanol. The rinsed pellet was resuspended in 50 μL of TE10.01 (10 mM Tris-HCl and 0.1 mM EDTA [pH 8]) containing 40 μg mL^{-1} heat-treated RNAseA. For DNA gel blots, the plant DNA was digested with restriction enzymes (Boehringer Mannheim/Roche, Basel) and separated on 0.7% (w/v) agarose gels. The DNA fragments were transferred in 0.4 N NaOH to Hybond N^+ nylon membranes and hybridized in 5× SSPE (0.9 M NaCl, 50 mM sodium phosphate, and 5 mM EDTA [pH 7.7]) at 65°C in the absence of formamide according to the instructions of the manufacturer (Amersham, Buckinghamshire, UK). The most stringent wash was in 0.1× SSC (15 mM NaCl and 1.5 mM sodium citrate) and 0.1% (w/v) SDS for 15 min at 65°C. Radioactive DNA probes were obtained with the Random Primed DNA Labeling Kit (Boehringer Mannheim/Roche).

Cloning of Genomic DNA

Genomic clones were obtained by three different methods: PCR (clones PC), genomic walk (clones GW), and library screen (clones LC). The following primers were used to amplify genomic DNA fragments by PCR: 2b (5′ GGCGGGGAAGAAGGGCTACAAGATGAAGAC 3′) and 2e (5′ CGATCTGCTGGCCATATCCTAAGAG 3′) for clone PC1-1 of *ZmPRPL35-1* and for clones of *ZmPRPL35-2* and *ZmPRPL35-3* (Fig. 4A) and 8516e (5′ ATTGCCTGTTTTAATAGCTGTACATAGAAA 3′) and 2M (5′ CGATGAATGCGTGAAGGATGGTAAAG 3′) for PC1-65 (Fig. 4A). Polymerase chain reactions were carried out in a GeneAmp PCR System 9700 (Perkin-Elmer Applied Biosystems, Foster City, CA) with an initial denaturation of 2 min at 94°C followed by 35 cycles of 30 s at 94°C, 1 min at 62°C, and 1 min at 72°C.

Genomic walk experiments were performed according to Devic et al. (1997) using nested gene-specific primers and genomic DNA of genotype A188 cut with enzymes *Dra*I, *Eco*RV, *Pvu*II, *Sca*I, or *Ssp*I. The PCR products were cloned in vector pGEM-T Easy (Promega, Madison, WI). The following primers/nested primers were used: GW3 (5′ GAAACTGGAAAGGCGAAATGGAGGGACG 3′)/GW3b (5′ GCTCGATAGGTTTATTGTGATAACGTTGCTGG 3′) for clone GW1-3 and GW4 (5′ GTCCCTCCATTTCGCCTTTCCAGTTTCC 3′)/GW4b (5′ CCAGCAACGTTATCACAATAAACCTATCGAGC 3′) for clone GW1-4 (Fig. 4A).

A genomic library of genotype HD5 × HD7 in vector λEMBL3 SP6/T7 (CLONTECH Laboratories, Palo Alto, CA) was screened with the radioactively labeled probe PC1-1 (Fig. 4A). DNA was isolated from single plaques and subcloned in vector pBluescript SK^+ or $pBCSK^+$ (Stratagene, La Jolla, CA). Clone LC1-13 (Fig. 4A) contained a 5.8-kb *Xba*I fragment with 2.05 kb upstream and 1.90 kb downstream of the ORF.

RT-PCR

Poly(A^+) RNA was isolated from appropriate tissues of genotype A188 using the Straight A's mRNA Isolation System (Novagen, Madison, WI) and treated with RQ1 RNase free DNase I (Promega). Approximately 100 ng was reverse transcribed in a final volume of 20 μL using an oligo(dT) primer and SuperScript II RNase H^- RT according to the manufacturer (Life Technologies/Gibco-BRL, Cleveland). Amplification of 1-μL aliquots involved an initial denaturation of 2 min at 94°C followed by a limiting number of cycles (18 for *Gapdh* and 25 for *ZmPRPL35*) of 1 min at 94°C, 1 min at 60°C, 1 min at 72°C, and a final extension of 5 min at 72°C. Ten-microliter aliquots of the PCR reaction were either digested with appropriate enzymes (Life Technologies/Gibco-BRL) or loaded directly on agarose gels. After electrophoresis, the gels were blotted and hybridized with radioactively labeled probes as described above. Individual bands were quantified using a STORM 840 PhosphorImager and ImageQuant software (Molecular Dynamics, Sunnyvale, CA). In control reactions, RT was replaced by water or reverse transcribed RNA by 20 ng of plasmid DNA of genomic clones. Primers 2b and 2e were used in standard RT-PCR, whereas primers RT5 and RT3 served for experiments involving SNPs.

Sequence Analysis

Template DNA was isolated with the QIAprep spin plasmid miniprep kit (Qiagen USA, Valencia, CA) and sent to Genome Express (Grenoble, France) for nucleotide sequence analysis. Nucleotide and amino acid sequences were compared with EMBL and GenBank databases using the BLAST algorithm (Altschul et al., 1997). Phylogenetic trees were constructed with the Clustal method (Higgins and Sharp, 1988) in the MEGALIGN module of the DNAstar program (Lasergene, Madison, WI). The genomic sequences re-

ported here were given the EMBL accession numbers AJ431185 (*ZmPRPL35-1*), AJ431188 (*ZmPRPL35-2*), and AJ431189 (*ZmPRPL35-3*), and the experimentally determined partial cDNA sequence was given the EMBL accession number AJ431193 (*ZmPRPL35-1*).

Consensus Sequences of Plant PRPL35 Proteins

The nucleotide and amino acid sequences of ZmPRPL35 were used for Blast searches of GenBank dbest. Nucleotide sequences with scores below e-4 were retained and assembled in contigs using the Sequencher software (GeneCodes, Ann Arbor, MI). The consensus sequence of each contig was translated in all three reading frames, and the amino acid sequence with the highest similarity to ZmPRPL35 was extracted. In the case of the rice (*Oryza sativa*) consensus sequence, several amino acid sequences in different reading frames were joined because of the poor quality of the nucleotide sequence. The consensus sequences were established from the following sequences: Arabidopsis EST with AA651266, AA720041, AC005170, AI999488, BE038795, BE039086, H36792, and X87332; barley (*Hordeum vulgare*) EST with BF266822 and BF627081; maize (*Zea mays*) EST with 33 sequences including AI001298, AI374506, AI586766, and BE761561; *Physcomitrella patens* EST 1 with AW497162 and AW561496; *P. patens* EST 2 with AW598801; potato (*Solanum tuberosum*) EST with AW096855; rice EST with AU057515 and AU057516; soybean (*Glycine max*) EST 1 with AW202231, AW782256, BE190178, BE210806, BE609189, BE609197, BE612269, and BE800236; soybean EST 2 with AW306546, AW734853, AW760237, AW781016, BE609020, BE801564, and BE806944; tomato (*Lycopersicon esculentum*) EST with AI780520, AW092994, and AW623869; and wheat (*Triticum aestivum*) EST with BE400782, BE425970, BE426812, BE488830, BE488831, BE488908, BE489001, BE489731, and BE497124.

DNA Gel Blots

For DNA gel blots, plant DNA, plasmid DNA, or PCR products were digested with restriction enzymes (Boehringer Mannheim/Roche) and separated on 0.7% (w/v) agarose gels. The DNA fragments were transferred in 0.4 N NaOH to Hybond N^+ nylon membranes and hybridized according to the instructions of the manufacturer (Amersham). Under "moderate" conditions, the most stringent wash was for 10 min in 0.2× SSC and 0.1% (w/v) SDS. Under "stringent" conditions, two additional washes for 15 min each were performed at 65°C in 0.1× SSC and 0.1% (w/v) SDS.

Radioactive DNA probes were obtained with the random-primed DNA labeling kit (Boehringer Mannheim/Roche). The most commonly used probe was the insert of plasmid pRT1-58. This plasmid resulted from cloning a RT-PCR product obtained on A188 embryos with primers 2b (5′ GGCGGGGAAGAAGGGCTACAAGATGAAGAC 3′) and 2e (5′ CGATCTGCTGGCCATATCCTAAGAG 3′) into the vector pGEM-T-Easy (Promega).

Mapping of RFLPs

Genomic clone PC1-65 or cDNA clone RT1-58 and were radioactively labeled and used as probes in DNA gel blots to identify RFLPs between the parents of the inbred mapping populations of Brookhaven National Laboratory (Burr and Burr, 1991) or Limagrain Genetics International (A. Murigneux, Clermont-Ferrand, France). The resulting polymorphisms were scored within the corresponding inbred populations, and the corresponding loci were placed on the current Brookhaven National Laboratory map using the MapMaker program (Lander et al., 1987). Gene *ZmPRPL35-1* is indexed as marker ensl014 on the current BNL map.

Maize Transformation

Maize transformation of inbred line A188 with *Agrobacterium tumefaciens* strain LBA4404 harboring a super-binary plasmid was essentially performed as described (Ishida et al., 1996). In particular, the composition of all media cited hereafter is detailed in this reference. The super-binary plasmid was the result of a recombination between plasmid L315 harboring between T-DNA borders a Basta resistance cassette and *ZmPRPL35-1* (5.8-kb *Xba*I fragment of pLC1-13) and plasmid pSB1 harboring the *virB* and *virG* genes isolated from the super-virulent strain A281. Immature embryos isolated at 10 DAP were incubated for 5 min with *A. tumefaciens* and cultured for 3 d on LSAs medium without selection in the dark at 25°C. Upon transfer to medium LSD5, *A. tumefaciens* was counter-selected by the presence of 250 mg L^{-1} cefotaxime, and transformed calli were selected by the presence of 5 mg mL^{-1} phosphinotricin. After 2 weeks of culture, developing calli were transferred to LSD10 medium containing 10 mg mL^{-1} phosphinotricin and cultured for 3 weeks. Type I calli were excised and cultured for another 3 weeks, maintaining the selective pressure. For regeneration, well-developed type I calli were cultured on LSZ medium at 22°C under selective pressure and continuous. After 2 weeks, shoots bearing calli were transferred to RMG2 medium and cultured another 2 weeks before their transfer to soil and gradual acclimatization to ambient humidity.

Confocal Microscopy

The preparation of embryos for confocal microscopy followed essentially the protocol of Braselton et al. (1996). Immature kernels were removed from the ear at defined developmental stages and cut into three equal slices along their longitudinal axis. The central slice was vacuum infiltrated on ice for 30 min with a mixture of ethanol:acetic acid (3:1 [v/v]). The fixative was renewed (2 mL per slice), and the tissues were incubated overnight at 4°C. The tissues were rinsed three times with water for 15 min each and hydrolyzed in 5 N HCl for 50 min at room temperature. After rinsing three times with water for 5 min each, the tissues were stained for 2 h with commercial Schiff reagent (Sigma, St. Louis). The samples were dehydrated in an ethanol series and transferred for 1 h into a 1:1 (v/v) mixture of ethanol:LR White acrylic resin (Sigma). After an overnight incubation in pure LR White, the embryos were dissected from the remaining tissues under a fume hood and collected in a drop of LR White on a glass slide. A cover slide was placed on top of the samples, and the resin was polymerized by overnight incubation at 60°C. The embryos were observed and photographed with a LSM510 confocal microscope (Zeiss, Jena, Germany).

Electron Microscopy

Immature embryos were dissected at defined developmental stages and fixed overnight at 4°C with 2% (v/v) glutaraldehyde in 0.1 M cacodylate buffer (pH 7) and postfixed for 2 h with OsO_4 in 0.1 M cacodylate buffer. The samples were postfixed in 2% (w/v) osmium tetroxide in the same buffer for 3 h at room temperature and rinsed for 1 h in the same buffer. After dehydration in an ethanol series, the samples were embedded in LR White acrylic resin (Sigma). Serial ultrathin sections were cut with a diamond knife on a Reichert Ultracut OMU3 microtome (Reichert, Wien, Australia). The sections were collected on formvar-coated grids and stained with uranyl acetate and lead citrate in an LKB Ultrostainer (LKB Produkter, Bromma, Sweden). Observations were made with an HU 12A electron microscope (Hitachi, Tokyo).

In Situ Hybridization

The methods for digoxygenin labeling of RNA probes, tissue preparation, and in situ hybridization were essentially as described by Coen et al. (1990) and Bradley et al. (1993). The *Kn1* and *LTP2* probes were gifts from Sarah Hake (Plant Gene Expression Center, Albany, Canada) and Pere Puigdomenech (Consejo Superior de Investigaciones Cientificas, Barcelona), respectively.

Biochemical Analysis of Maize Kernels

For biochemical analysis pools of hand-selected wild-type and *emb8516* kernels were sent to the Vendome Experimental Station of the Institut Technique des Céréales et des Fourrages (Pouline, France) where standard methods were used for the quantification of reserve substances. Because the embryo accounts for 13% of the dry matter of the kernel (Landry and Moureaux, 1980), the original values in grams per kilogram dry matter were normalized for *emb* kernels but not for wild-type kernels. The values of *emb* kernels in Table I present 87% of the original value.

ACKNOWLEDGMENTS

We thank Bill Sheridan for the isolation of the *emb8516* mutant and invaluable advice throughout the project. We thank Régis Mache for fruitful discussion, Michel Beckert for the use of the Institut National de la Recherche Agronomique field facilities, and Ben Burr and Alain Murigneux for their recombinant inbred lines and the analysis of our RFLP data. Frédéric Berger and Jean-Emmanuel Faure are acknowledged for advice on confocal microscopy, Nathalie Frangne for help with electron microscopy, and Olivier Sellam for scoring of mutant ears. Sarah Hake furnished the *Knotted1* probe, and Pere Puigdomenech provided the *LTP2* probe. Alexis Lacroix, Armand Guillermin, and Hervé Leyral provided excellent technical assistance.

Received July 24, 2003; returned for revision October 10, 2003; accepted November 10, 2003.

LITERATURE CITED

Aalen RB, Opsahl-Ferstad H-G, Linnestad C, Olsen O-A (1994) Transcripts encoding an oleosin and a dormancy-related protein are present in both the aleurone layer and the embryo of developing barley (*Hordeum vulgare* L.) seeds. Plant J **5:** 385–396

Albert S, Despres B, Guilleminot J, Bechtold N, Pelletier G, Delseny M, Devic M (1999) The EMB 506 gene encodes a novel ankyrin repeat containing protein that is essential for the normal development of Arabidopsis embryos. Plant J **17:** 169–179

Altschul SF, Madden TL, Schäfer AA, Zhang J, Zhang E, Miller W, Lipman DJ (1997) Gapped BLAST and PSI-BLAST: a new generation of protein database search programs. Nucleic Acid Res **25: 3389–3402**

Apuya NR, Yadegari R, Fischer RL, Harada JJ, Goldberg RB (2002) RASPBERRY3 gene encodes a novel protein important for embryo development. Plant J **129:** 691–705

Apuya NR, Yadegari R, Fischer RL, Harada JJ, Zimmerman JL, Goldberg RB (2001) The *Arabidopsis* embryo mutant *schlepperless* has a defect in the *chaperonin-60alpha* gene. Plant Physiol **126:** 717–730

Barloy D, Denis L, Beckert M (1989) Comparison of the aptitude for anther culture in some androgenetic doubled haploid maize lines. Maydica **34:** 303–308

Bradley D, Carpenter R, Sommer H, Hartley N, Coen E (1993) Complementary floral homeotic phenotypes result from opposite orientations of a transposon at the *plena* locus of *Antirrhinum*. Cell **72:** 85–95

Braselton JP, Wilkinson MJ, Clulow SA (1996) Feulgen staining of intact plant tissues for confocal microscopy. Biotechnol Histochem **71:** 84–87

Burr B, Burr FA (1991) Recombinant inbreds for molecular mapping in maize: theoretical and practical considerations. Trends Genet **7:** 55–60

Clark JK, Sheridan WF (1991) Isolation and characterisation of 51 *embryo-specific* mutations of maize. Plant Cell **3:** 935–951

Coen ES, Romero JM, Doyle S, Elliott R, Murphy G, Carpenter R (1990) *floricaula*: a homeotic gene required for flower development in *Antirrhinum majus*. Cell **63:** 1311–1322

Dabbs ER (1991) Mutants lacking individual ribosomal proteins as a tool to investigate ribosomal properties. Biochimie **73:** 639–645

Devic M, Albert S, Delseny M, Roscoe TJ (1997) Efficient PCR walking on plant genomic. DNA. Plant Physiol Biochem **35:** 331–339

Dominguez F, Moreno J, Cejudo FJ (2001) The nucellus degenerates by a process of programmed cell death during the early stages of wheat grain development. Planta **213:** 352–360

Elster R, Bommert P, Sheridan WF, Werr W (2000) Analysis of four *embryo-specific* mutants in *Zea mays* reveals that incomplete radial organisation of the proembryo interferes with subsequent development. Dev Genes Evol **210:** 300–310

Friedman WE (1994) The evolution of embryogeny in seed plants and the developmental origin and early history of endosperm. Am J Bot **81:** 1468–1486

Gerdes JT, Tracy WF (1993) Pedigree diversity within the Lancaster surecrop heterotic group of maize. Crop Sci **33:** 334–337

Heckel T, Werner K, Sheridan WF, Dumas C, Rogowsky PM (1999) Novel phenotypes and developmental arrest in early *embryo specific* (*emb*) mutations of maize. Planta **210:** 1–8

Helentjaris T (1995) Atlas of duplicated sequences. Maize Genet Coop Newslett **69:** 67–82

Higgins DG, Sharp PM (1998) CLUSTAL: a package for performing multiple sequence alignment on a microcomputer. Gene **73:** 237–244

Horiguchi G, Kodama H, Iba K (2003) Mutations in a gene for plastid ribosomal protein S6-like protein reveal a novel developmental process required for the correct organization of lateral root meristem in Arabidopsis. Plant J **33:** 521–529

Ingram GC, Boisnard-Lorig C, Deguerry F, Dumas C, Rogowsky PM (2000) Expression patterns of genes encoding HD-ZipIV homeodomain proteins define specific domains in the maize embryos and meristems. Plant J **22:** 401–414

Ishida Y, Saito H, Ohta S, Hiei Y, Komari T, Kumashiro T (1996) High efficiency transformation of maize (*Zea mays* L.) mediated by *Agrobacterium tumefaciens*. Nat Biotechnol **14:** 745–750

Jürgens G (2001) Apical-basal pattern formation in *Arabidopsis* embryogenesis. EMBO J **20:** 3609–3616

Kaplan DR, Cooke TJ (1997) Fundamental concepts in the embryogenesis of dicotyledons: a morphological interpretation of embryo mutants. Plant Cell **9:** 1903–1919

Lander ES, Green P, Abrahamson J, Barlow A, Daly MJ, Lincoln SE, Newburg L (1987) MAPMAKER: an interactive computer package for constructing primary genetic linkage maps of experimental and natural populations. Genomics **1:** 174–181

Landry J, Moureaux T (1980) Distribution and amino acid composition of protein groups located in different histological parts of maize grain. J Agric Food Chem **28:** 1186–1191

Lid SE, Gruis D, Jung R, Lorentzen JA, Ananiev E, Chamberlin M, Niu X, Meeley R, Nichols S, Olsen OA (2002) The *defective kernel 1* (*dek1*) gene required for aleurone cell development in the endosperm of maize grains encodes a membrane protein of the calpain gene superfamily. Proc Natl Acad Sci USA **99:** 5460–5465

Neuffer MG, Sheridan WF (1980) Defective kernel mutants of maize: I. Genetic and lethality studies. Genetics **95:** 929–944

Opsahl-Ferstad HG, Le Deunff E, Dumas C, Rogowsky PM (1997) *ZmEsr*, a novel endosperm-specific gene expressed in a restricted region around the maize embryo. Plant J **12:** 235–246

Pesaresi P, Varotto C, Meurer J, Jahns P, Salamini F, Leister D (2001) Knock-out of the plastid ribosomal protein L11 in *Arabidopsis*: effects on mRNA translation and photosynthesis. Plant J **27:** 179–189

Sambrook J, Fritsch EF, Maniatis T (1989) Molecular Cloning: A Laboratory Manual. Cold Spring Harbor Laboratory Press, Cold Spring Harbor, NY

Schultes NP, Sawers RJ, Brutnell TP, Krueger RW (2000) Maize *high chlorophyll fluorescent 60* mutation is caused by an *Ac* disruption of the gene encoding the chloroplast ribosomal small subunit protein 17. Plant J **21:** 317–327

Schwartz B, Yeung E, Meinke D (1994) Disruption of morphogenesis and transformation of the suspensor in abnormal suspensor mutants of *Arabidopsis*. Development **120:** 3235–3245

Sheridan WF, Clark JK (1993) Mutational analysis of morphogenesis of the maize embryo. Plant J **3:** 347–358

Sheridan WF, Neuffer MG (1980) Defective kernel mutants of maize: II. Morphological and embryo culture studies. Genetics **95:** 945–960

Smith LG, Jackson D, Hake S (1995) Expression of *knotted1* marks shoot meristem formation during maize embryogenesis. Dev Genet **16:** 344–348

Smooker PM, Choli T, Subramanian AR (1990) Ribosomal protein L35: identification in spinach chloroplasts and isolation of a cDNA clone encoding its cytoplasmic precursor. Biochemistry **29:** 9733–9736

Sossountzov L, Ruiz-Avila L, Vignols F, Jolliot A, Arondel V, Tchang F, Grosbois M, Guerbette F, Miginiac E, Delseny M et al. (1991) Spatial and temporal expression of a maize lipid transfer protein gene. Plant Cell **3:** 923–933

Stiefel V, Becerra EL, Roca R, Bastida M, Jahrmann T, Graziano E, Puigdomenech P (1999) TM20, a gene coding for a new class of transmembrane proteins expressed in the meristematic tissues of maize. J Biol Chem **274:** 27734–27739

Taiz L, Zeiger E (1998) Plant Physiology. Sinauer Associates Inc., Sunderland, MA

Uwer U, Willmitzer L, Altmann T (1998) Inactivation of a glycyl-tRNA synthetase leads to an arrest in plant embryo development. Plant Cell **10:** 1277–1294

Van Lammeren AAM (1987) Embryogenesis in *Zea mays* L.: a structural approach to maize caryopsis development in vivo and in vitro. Plant Cytology and Morphology. Agricultural University Wageningen, The Netherlands, p 175

Weber H, Borisjuk L, Wobus U (1997) Sugar import and metabolism during seed development. Trends Plant Sci **2:** 169–174

Woo HR, Goh CH, Park JH, de la Serve BT, Kim JH, Park YI, Nam HG (2002) Extended leaf longevity in the ore4–1 mutant of Arabidopsis with a reduced expression of a plastid ribosomal protein gene. Plant J **31:** 331–340

Yadegari R, de Paiva GR, Laux T, Koltunow AM, Apuya N, Zimmerman JL, Fischer RL, Harada JJ, Goldberg RB (1994) Cell differentiation and morphogenesis are uncoupled in *Arabidopsis raspberry* embryos. Plant Cell **6:** 1713–1729

Yamaguchi K, Subramanian AR (2000) The plastid ribosomal proteins. Identification of all the proteins in the 50 S subunit of an organelle ribosome (chloroplast). J Biol Chem **275:** 28466–28482

Yamaguchi K, von Knoblauch K, Subramanian AR (2000) The plastid ribosomal proteins: identification of all the proteins in the 30 S subunit of an organelle ribosome (chloroplast). J Biol Chem **275:** 28455–28465

Young TE, Gallie DR (2000) Programmed cell death during endosperm development. Plant Mol Biol **44:** 283–301